Final Draft
Manuscript available at: https://doi.org/10.1061/(ASCE)ST.1943-541X.0001445
Full citation: Ballard, ZC, Thrall, AP, Smith, BJ, and Casias, CM (2016) "Impact of Hinged Connectors on Sandwich Panel Behavior." Journal of Structural Engineering, 142(3), 06015005

Impact of Hinged Connectors on Sandwich Panel Behavior

Zach C. Ballard, [1]; Ashley P. Thrall, A.M.ASCE [2]; Brian J. Smith, P.E. [3]; Casey M. Casias, S.M.ASCE [4];

ABSTRACT

This paper discusses the impact of hinged connectors (a common connection in folding structures) on the behavior of sandwich panels (with fiber-reinforced polymer faces and foam core). A sandwich panel is subjected to uniform loading and tested when restrained by hinged connectors in compression and in tension. The measured results are compared to finite element numerical models, focusing on global behavior (displacements and strains at center) and local behavior (strains near connectors). Parametric studies using these validated numerical models investigate the impact of the number, size, and relative placement of hinged connectors. These studies culminate in guidelines for the design of structures comprised of hinged, folding panels. Ultimately, this paper addresses a research gap in understanding the behavior of sandwich panels connected by hinges.

CE Database subject headings: Sandwich panels; Hinges; Connections

INTRODUCTION

Sandwich panels are often used in shipping, aerospace, automotive, and construction industries where lightweight, high-strength materials are necessary. When connected by hinges, they can be utilized for folding, deployable structures where a small packaged volume and low self-weight are required for transportation (Quaglia et al., 2014).

[1]Postdoctoral Research Associate, Kinetic Structures Laboratory, Department of Civil and Environmental Engineering and Earth Sciences, University of Notre Dame, Notre Dame, IN 46556. E-mail: zballard@nd.edu

[2]Myron and Rosemary Noble Assistant Professor of Structural Engineering, Kinetic Structures Laboratory, Department of Civil and Environmental Engineering and Earth Sciences, University of Notre Dame, Notre Dame, IN 46556. (corresponding author) E-mail: athrall@nd.edu

[3]Assistant Teaching Professor and Research Engineer, Kinetic Structures Laboratory, Department of Civil and Environmental Engineering and Earth Sciences, University of Notre Dame, Notre Dame, IN 46556. E-mail: bsmith24@nd.edu

[4]Graduate Student, Kinetic Structures Laboratory, Department of Civil and Environmental Engineering and Earth Sciences, University of Notre Dame, Notre Dame, IN 46556. E-mail: ccasias@nd.edu

A wide body of experimental research has been performed to better understand the properties of isolated sandwich panels, including flexural strength [e.g., Manalo et al. (2010), Kesler and Gibson (2002), Daniel and Abot (2000)], compressive strength [e.g, Malcom et al. (2013), Mamalis et al. (2005)], and characterization of failure modes [e.g., Russo and Zuccarello (2006)]. Fasteners/inserts play a key role in the strength and stiffness of sandwich panels and have been investigated both experimentally and numerically [e.g., Heimbs and Pein (2009), Bunyawanichakul et al. (2005), Demelio et al. (2001), De Matteis and Landolfo (1999a)]. Despite the large number of research studies, the majority of past experimental work has been limited to understanding the behavior of individual components. There have been few experimental or numerical studies on structures comprised of multiple sandwich panels or panel-to-panel connections [e.g., Dawood and Peirick III (2013), Heimbs and Pein (2009), De Matteis and Landolfo (1999a), De Matteis and Landolfo (1999b)].

The objective of this research is to address the existing knowledge gap in understanding the impact of hinged connectors on the behavior of structures comprised of sandwich panels. A single sandwich panel [comprised of fiber-reinforced polymer (FRP) faces and a foam core] is experimentally tested under a uniformly distributed surface pressure (emulating wind loads) when the sample is restrained by hinged connectors in compression and in tension (as separate tests). The measured results are compared to finite element numerical models, focusing on the panel displacements and surface strains. These validated numerical models are used to perform parametric studies investigating the impact of the number, size, and relative placement of hinged connectors. These studies culminate in guidelines for the design of structures comprised of hinged, folding panels.

MATERIAL PROPERTIES

Material properties of the FRP face and foam core of the sandwich panel were measured according to the applicable ASTM standards using an Instron 5590 Universal Testing Machine (Table 1). The 1.78 mm (0.07 in.) thick FRP faces are comprised of Vectorply biaxial (E-LT 1200-P) and double-bias (E-BX 1200) e-glass laminate (layup: 0°/90°/45°/-45°/-45°/45°/90°/0°) (Vectorply, 2002) with vinyl ester resin. The 31.8 mm (1.25 in.) core is Corecell M80 Foam (Gurit, 2013).

EXPERIMENTAL PROGRAM

A single sandwich panel was tested under two scenarios: (1) hinges in compression, where the panel is restrained by hinges loaded in compression (Figure 1a-c) and (2) hinges in tension, where the panel is restrained by hinges loaded in tension (Figure 1d-f). The panel was 1100 mm (43.5 in.) long by 1070 mm (42 in.) wide. Panel end caps increased the face thickness to 4.95 mm (0.195 in.) near the panel edges. The panel featured three aluminum (alloy type 5052) hinges along each transverse edge that were 76.2 mm (3.00 in) long and 2.54 mm (.100 in) thick with a 6.35 mm (.250 in.) diameter pin, and an open leaf width of 76.2 mm (3.00 in.). Hinges were placed at panel center and 114 mm (4.5 in.) from each edge in the transverse direction, inset 65.1 mm (2.56 in) from each edge in the longitudinal direction (Figure 2). In both tests, the panel was aligned parallel to the ground at an approximate height of 127 mm (5.00 in.) and subjected to an increasing uniformly distributed surface load designed to emulate wind pressure [up to 1.44 kPa (30.0 psf)]. The load was applied to the surface of the panel via an urethane film air bladder [813 mm (32.0 in.) by 1120 mm (44.0 in.)] placed underneath the panel. For the hinges in compression test, eyebolts connected the panel hinges to elevated W6x12 steel beams (Figure 1c) that served as a rigid reaction frame. For the hinges in tension test, eyebolts were used to connect the panel hinges to the floor via steel base plates (Figure 1f).

Midline panel displacements were measured by three displacement transducers (MD Totco 1850-002, string pots) attached to a W6x12 steel beam used as a stationary reference frame. Up to 18 strain gages (MicroMeasurements N2A-00-10CBE-350) were adhered to the panel to measure longitudinal and transverse surface strains (Figure 2). The pressure from the air bladder on the panel was measured using a pressure sensor (Omega PX409) placed in-line with the air tubes used to inflate the bladder. Note that reported applied pressure refers to the pressure increase above the internal air bladder pressure at full contact with the panel [at 0.96 kPa (20.0 psf)]. The corresponding displacements and surface strains are reported. This does not include the displacements and strains due to self-weight and that occurred during the uneven inflation of the air bladder prior to full contact (since the degree of bladder contact during the inflation process could not be measured or numerically simulated).

NUMERICAL MODELING

Three-dimensional finite element numerical models were developed using ABAQUS (ABAQUS, 2013). The FRP faces were modeled using S4R shell elements while the foam core was modeled using C3D8R solid elements using a linear-elastic stress-strain relationship based on the measured material properties (Table 1). Each face was continuously tied to the core surface. A single leaf for each hinge was modeled as a rectangular aluminum (alloy type 5052) S4R shell element [assumed material properties: E=70.330 MPa (10,200 ksi), ρ=2680 $\frac{kg}{m^3}$ (168 $\frac{lb}{ft^3}$)]. The hinge leafs were tied to the panel end caps at three distinct nodes to match the fastener locations of each leaf to the panel. A mesh size of 12.7 mm (0.500 in.) was used to ensure numerical convergence.

Boundary conditions were applied along lines located at the outer edge of each hinge, corresponding to the location of the barrel (or rotation mechanism of the hinge). Models were created for pin-roller, pin-pin, and fix-fix boundary conditions applied along this restraint line. The pin-roller and pin-pin models were used to assess the observed relative translation permitted in the hinged connectors and the fix-fix boundary conditions were used to investigate the effects of long-term use in which hinges may become locked due to debris or corrosion. Note that the model for the hinges in compression test features the hinges on the tension (i.e., top) face of the panel while the model for the hinges in tension test features the hinges on the compression (i.e., bottom) face of the panel. A uniformly distributed upward pressure was applied to the entire surface of the panel to emulate the applied pressure from the air bladder after the bladder was fully in-contact with the panel.

RESULTS

Hinges in Compression Test

Figures 3a and 3b show a comparison of the measured global (displacements and strains at center) behavior of the hinges in compression test with numerical models featuring pin-roller, pin-pin, and fix-fix hinge barrel boundary conditions. The measured displacements and the longitudinal surface strains at the center of the panel closely match the pin-roller hinge barrel boundary condition model, indicating that hinges permit some horizontal translation of the panel (i.e., internal movement of the barrel). If this horizontal translation becomes limited in the field (pin-pin conditions) or if rotation is also restrained (fix-fix condition), the global load-displacement behavior becomes stiffer.

Considering the local behavior (strains near connectors), the pin-roller hinge barrel boundary condition provides an excellent prediction for the measured surface strains at all hinge locations (Figure 3c). If a pin-pin hinge barrel boundary condition were to occur over long-term use due to accumulation of debris or corrosion within the hinge, the strains are predicted to become compressive and increase dramatically in magnitude (Figure 3c). If a fix-fix condition occurs, this effect is observed to a slightly lesser degree. Based on these results, it is recommended that designers evaluate hinges as pin-roller, pin-pin, and fix-fix conditions to obtain an envelope of possible local strains. Additional reinforcing (e.g., thickening of FRP) in these regions may be warranted.

Hinges in Tension Test

Figures 4a and 4b show a comparison of the global measured behavior of the hinges in tension test with numerical models featuring pin-roller, pin-pin, and fix-fix hinge barrel boundary conditions. The measured center displacements (Figure 4a) more closely resemble the pin-roller model, while the longitudinal surface strains at the center of the panel (Figure 4b) are stiffer than predictions from all three numerical models. This can be attributed to approximations in modeling the core. The sample panel core is impregnated with small columns of vinyl ester resin during manufacturing. This added stiffness is not accounted for in the numerical model. This effect is more noticeable in the hinges in tension test since the supports are on the opposite face to the measured strain; therefore, the core plays a larger part in the behavior. Consistent with the hinges in compression test, the fix-fix and pin-pin hinge barrel boundary conditions result in stiffer behavior.

As in the hinges in compression test, the most significant effect of the hinge barrel boundary conditions can be seen in the localized longitudinal surface strains (Figure 4c). These strains are measured on the same face as the support; therefore they are not significantly affected by the modeling of the core. In general, the pin-roller hinge barrel boundary condition provides an excellent prediction for the measured surface strains. The pin-pin condition changes the strains from compressive to tensile and significantly increases the magnitude (consistent with findings from the hinges in compression test). A similar effect occurs in the fix-fix condition, though to a lesser extent. An exception occurs at Corner A - Right (upper right plot in Figure 4c) where the measured results are between the pin-roller and the pin-pin/fix-fix conditions. This discrepancy is likely due to the relative allowable movement in the hinge near Corner A - Right, which underscores the importance of designers evaluating pin-roller, pin-pin, and fix-fix hinge barrel boundary conditions.

PARAMETRIC STUDY OF THE NUMBER, SIZE, AND PLACEMENT OF HINGED CONNECTORS

The comparisons between the measured and numerical results validated the numerical models for use in a parametric study assessing the impact of the number (Figure 5), size (Figure 6), and relative placement (Figure 7) of hinged connectors on both global and local behavior (Ballard et al., 2015). The hinges in compression numerical model was used for all results with pin-roller hinge barrel boundary conditions since the numerical predictions more closely matched the measured behavior than the hinges in tension model. Minor revisions to the numerical model to isolate the effect of changes in the hinged connectors include (1) extending the longitudinal width of the end caps to 116 mm (4.56 in.) along the full transverse length, and (2) continuously tying hinge leafs to the surface as opposed to three discrete locations within the hinge leaf that corresponded to fastener locations. To fully capture local behavior, the reported strain corresponds to the local maximum in the end cap near the hinges, as this would be the region prone to failure.

Impact of Number of Hinged Connectors

Figure 5 compares the global behavior (i.e., midline and maximum displacements, Figure 5a and 5b) and local behavior (i.e., longitudinal strains near hinges in the end cap, Figure 5c and 5d) of varying the number of hinges. This parametric study included four models featuring from one to four hinges [38.1 mm (1.50 in.) wide x 76.2 mm (3.00 in.) long x 2.54 mm (.100 in.) thick, i.e., hinge size in sample] spaced approximately equidistant along each transverse edge, and a fifth model featuring a single continuous hinge.

As expected, more hinges result in stiffer panel behavior as shown by decreased midline displacements (Figure 5a). However, there is effectively no added benefit in increasing beyond 3 hinges (Figure 5b). Further, increasing the number of hinges, and especially the use of a continuous hinge, reduces the magnitude of local compressive strain concentrations (Figure 5c). However, there is again limited added benefit in implementing more than three hinges (Figure 5d). Based on these results, it is recommended that a hinge-number to transverse-length ratio of approximately 3.0 per meter balances the benefits of improved behavior with the added expense and weight of additional/continuous hinges.

Impact of Size of Hinged Connectors

Figure 6 shows the effect of hinge leaf length (see Figure 2 for definition) on (1) global behavior indicated by midline and maximum displacements (Figure 6a and 6b) and (2) local behavior indicated by longitudinal strains near hinges in the end cap (Figure 6c and 6d). Based on the above discussed results, all numerical models in this subsection feature three hinge connectors on each edge in the locations shown in Figure 2.

As expected, increasing the hinge length reduces the midline panel displacements (Figure 6a). While the continuous hinge shows the smallest displacements, the difference between continuous and the discrete hinges of varying lengths is insignificant in magnitude (Figure 6b). Local zones of high compressive strains are reduced as the hinge leaf lengthens (Figure 6c). The magnitude of this effect reduces with larger hinge lengths [i.e., the decrease in strain from the 76.2 mm (3.00 in.) to 152 mm (6.00 in.) hinge is less than that from 38.1 mm (1.50 in.) to 76.2 mm (3.00 in.)]. While longer hinge lengths, particularly the use of continuous hinges, improve local behavior, there is additional cost and weight associated with this design decision. To balance these priorities, designers should aim for a ratio of total-hinge-length (i.e., sum of lengths of all three hinges on one edge) to transverse-length ratio of around 0.2 [approximately that of the 76.2 mm (3.00 in.) hinge leaf investigated here].

The hinge width and thickness have negligible impact on the panel behavior [see Ballard et al. (2015)]. Therefore, the hinge width should be limited to the dimension necessary for secure fastening to the panel. Similarly, the hinge leaf thickness should be as thin as possible while meeting the required demands.

Impact of Relative Placement of Hinged Connectors

Figure 7 shows the impact of varying the distance between the center hinge and the outer hinges (identified in Figure 2) on the panel behavior. Based on the above discussed results, each model includes three hinges per side, with each hinge being 38.1 mm (1.50 in.) wide x 76.2 mm (3.00 in.) long x 2.54 mm (.100 in.) thick.

As expected, as the hinges are spaced further apart, the maximum midline panel deflections become smaller and deflections along the length of the panel become more uniform (Figure 7a and 7b). As the hinges move to the center, the displacement significantly increases, especially at the panel ends. Similarly, the surface compressive strains are reduced as the hinges are spaced further apart (Figure 7c), approximately linearly with the hinge distance (Figure 7d). For favorable panel behavior, designers should aim to place hinges equidistant along the panel edge.

Guidelines for Design

Based on this parametric study, the following guidelines for the design of sandwich panels connected by hinges are recommended:

- Select a hinge-number to transverse-length ratio of approximately 3.0 per meter to balance improved performance with the cost/weight of hinges.
- Select a hinge-length to transverse-length ratio of 0.2 to balance improved performance with cost/weight of hinges.
- Limit hinge width to that needed for secure fastening to the panel.
- Limit hinge thickness to meet the required demands.
- Space hinges equidistant for smaller and more uniform panel displacements with reduced local surface strains

These design guidelines are intended as qualitative guidelines for preliminary design. A detailed analysis and design would be required for a specific project.

CONCLUSIONS

This paper discussed the impact of hinged connectors (a common connection in folding structures) on the behavior of a representative sandwich panel (comprised of FRP faces and a foam core). The sandwich panel was subjected to a uniformly applied distributed load emulating wind pressures. Both experimental and numerical studies (using finite element models created in ABAQUS) were conducted to better understand the global and local panel behavior, with measured and predicted comparisons focusing on the panel displacements and longitudinal surface strains. Validated numerical models were then used to perform parametric studies, culminating in qualitative guidelines for design. Overall, this paper addresses a research gap in understanding the behavior of sandwich panels that feature hinged connectors.

ACKNOWLEDGEMENTS

This material is based upon work supported by the US Army Natick Soldier Research, Development and Engineering Center (NSRDEC) under Contract W911QY-12-C-0128.

REFERENCES

ABAQUS (2013). "ABAQUS/Standard Analysis User's Manual Version 6.13. Dassault Systemes, Waltham, MA.

Ballard, Z. C., Thrall, A. P., and Smith, B. J. (2015). "Parametric study of the effect of hinged connectors on the behavior of origami-inspired structures comprised of sandwich panels." *Proceedings of the ASME 2015 International Design Engineering Technical Conferences & Computers and Information in Engineering Conference*. Boston, MA.

Bunyawanichakul, P., Castanie, B., and Barrau, J. J. (2005). "Experimental and numerical analysis of inserts in sandwich panels." *Applied Composite Materials*, 12(3-4), 177–191.

Daniel, I. M. and Abot, J. L. (2000). “Fabrication, testing and analysis of composite sandwich beams.” *Composites Science and Technology*, 60(12-13), 2455–2463.

Dawood, M. and Peirick III, L. (2013). “Connection development and in-plane response of glass fiber reinforced polymer sandwich panels with reinforced cores.” *Canadian Journal of Civil Engineering*, 40(11), 1117–1126.

De Matteis, G. and Landolfo, R. (1999a). “Mechanical fasteners for cladding sandwich panels: Interpretative models for shear behaviour.” *Thin-Walled Structures*, 35(1), 61–79.

De Matteis, G. and Landolfo, R. (1999b). “Structural behaviour of sandwich panel shear walls: An experimental analysis.” *Materials and Structures*, 32(219), 331–341.

Demelio, G., Genovese, K., and Pappalettere, C. (2001). “An experimental investigation of static and fatigue behavior of sandwich composite panels joined by fasteners.” *Composites Part B: Engineering*, 32(4), 299–308.

Gurit (2013). “Corecell M-foam - the marine foam. http : //www.gurit.com/files/documents/corecell − m − foamv5pdf.pdf (October 9, 2013).

Heimbs, S. and Pein, M. (2009). “Failure behavior of honeycomb sandwich corner joints and inserts.” *Composite Structures*, 89(4), 575–588.

Kesler, O. and Gibson, L. J. (2002). “Size effects in metallic foam core sandwich beams.” *Materials Science and Engineering A*, A326, 228–234.

Malcom, A. J., Aronson, M. T., Deshpande, V. S., and Wadley, H. N. G. (2013). “Compressive response of glass fiber composite sandwich structures.” *Composites Part A: Applied Science and Manufacturing*, 54, 88–97.

Mamalis, A. G., Manolakos, D. E., Ioannidis, M. B., and Papapostolou, D. P. (2005). “On the crushing response of composite sandwich panels subjected to edgewise compression: Experimental.” *Composite Structures*, 71(2), 246–257.

Manalo, A. C., Aravinthan, T., Karunasena, W., and Islam, M. M. (2010). “Flexural behaviour of structural fibre composite sandwich beams in flatwise and edgewise positions.” *Composite Structures*, 92(4), 984–995.

Quaglia, C. P., Dascanio, A. J., and Thrall, A. P. (2014). “Bascule shelters: A novel erection strategy for origami-inspired structures.” *Engineering Structures*, 75, 276–287.

Russo, A. and Zuccarello, B. (2006). “Experimental and numerical evaluation of the mechanical behaviour of GFRP sandwich panels.” *Composite Structures*, 81(4), 575–586.

Vectorply (2002). “Laminated properties and packaging. $\mathrm{http://www.vectorply.com/ri-laminateprop.html}$ (November 29, 2014).

List of Tables

TABLE 1: Measured material properties of sandwich panel components.

	Panel Core					Panel Face			
Property	ρ_c (kg/m^3)	E_c (MPa)	σ_c (MPa)	τ_c (MPa)	G_c (MPa)	ρ_f (kg/m^3)	E_f (MPa)	σ_f (MPa)	ν_f
Mean	87.5	57.7	1.25	1.56	47.2	1740	15500	283	0.261
Std. Dev.	0.833	2.44	9.86e-3	9.45e-3	2.16	5.20	737	17.0	0.0145
COV	0.950%	4.23%	0.790%	6.03%	4.59%	0.299%	4.76%	6.02%	5.55%
ASTM Standard	C271	C365		C393	D7250	D792	D3039		
No. of Samples	10	10	10	5	5	5	8	5	8

Note: Subscripts c and f correspond to sandwich panel core and face, respectively. ρ = density, E = elastic modulus, G = shear modulus, τ = shear strength, σ = ultimate strength, ν = Poisson's ratio, Std. Dev. = standard deviation, and COV = coefficient of variation.

List of Figures

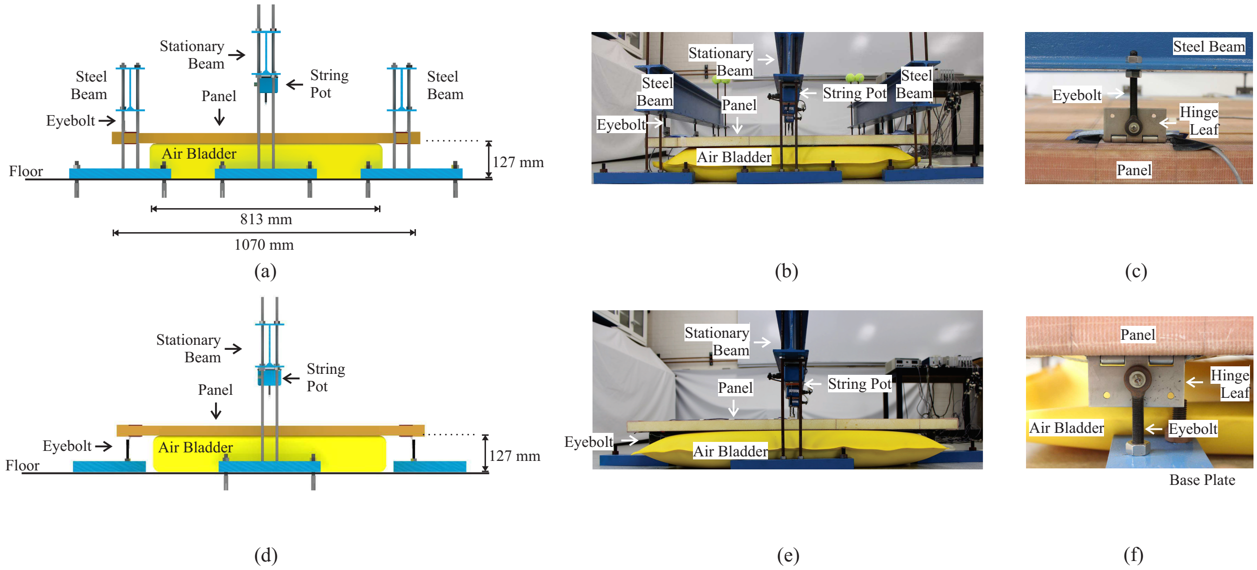

FIG. 1: Hinges in compression test: (a) elevation view, (b) photograph, and (c) hinged connector photograph; Hinges in tension test: (d) elevation view, (e) photograph and (f) hinged connector photograph.

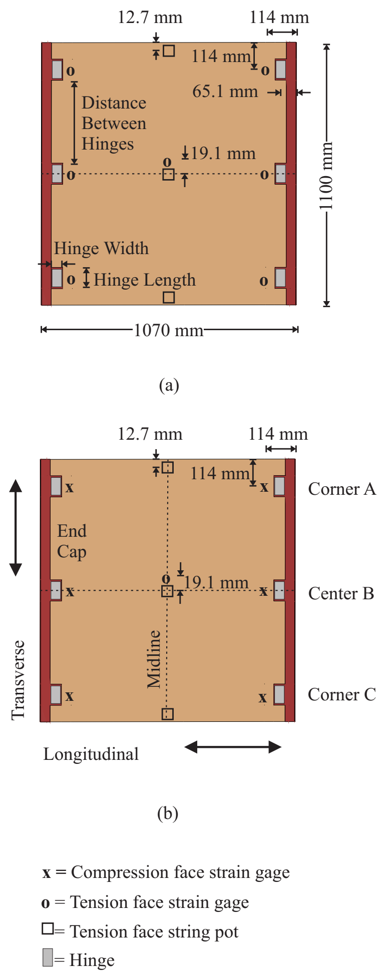

FIG. 2: Plan view of measurement system locations for (a) hinges in compression test and (b) hinges in tension test.

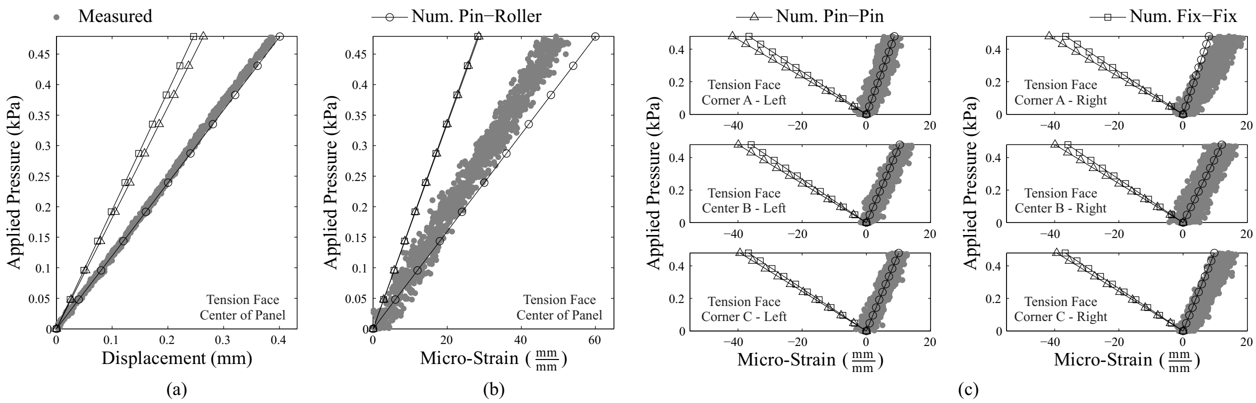

FIG. 3: Measured and numerical behavior (tension face) for hinges in compression test: (a) global displacements (center of panel), (b) global longitudinal strains (center of panel), and (c) localized longitudinal strains near hinges.

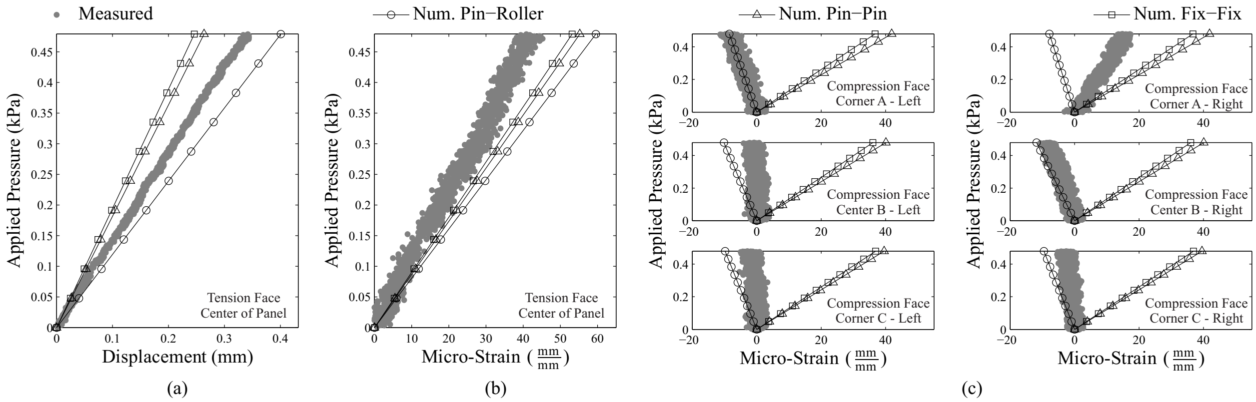

FIG. 4: Measured and numerical behavior for hinges in tension test: (a) global displacements (tension face, center of panel), (b) global longitudinal strains (tension face, center of panel), and (c) localized longitudinal strains near hinges (compression face).

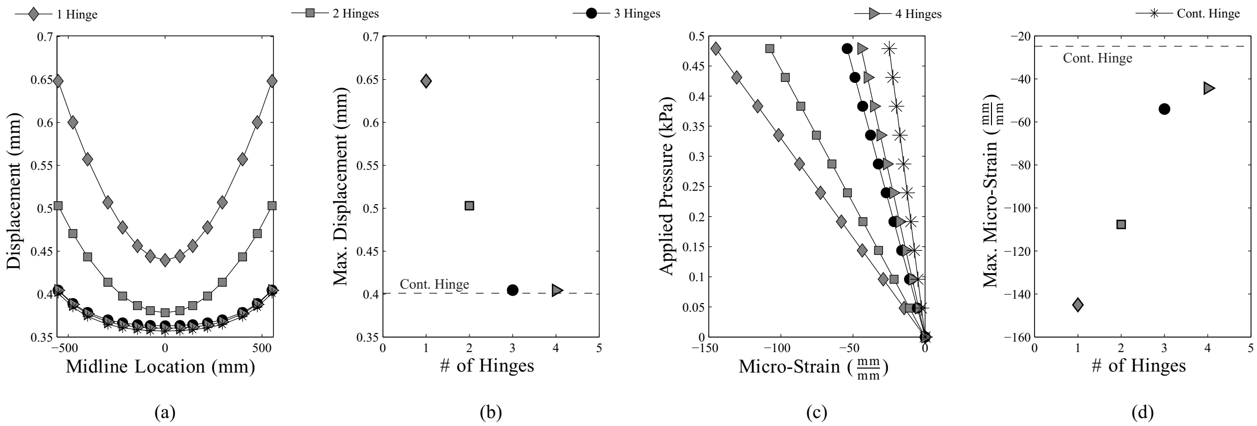

FIG. 5: Numerical behavior of panel (tension face) with varying number of hinged connectors: (a) global displacements along panel midline at an applied pressure of 0.479 kPa, (b) maximum displacement at an applied pressure of 0.479 kPa, (c) longitudinal strain near hinge, and (d) maximum longitudinal strain near hinge at an applied pressure of 0.479 kPa. Reprinted from Ballard et al. (2015), permission request pending.

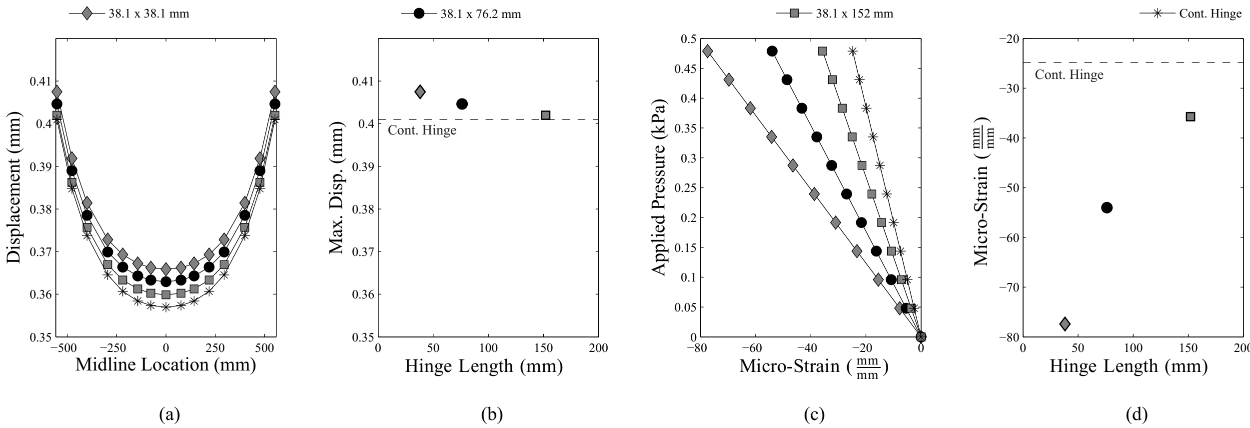

FIG. 6: Numerical behavior of panel (tension face) with varying length of hinged connectors: (a) global displacements along panel midline at an applied pressure of 0.479 kPa, (b) maximum displacement at an applied pressure of 0.479 kPa, (c) longitudinal strain near hinge, and (d) maximum longitudinal strain near hinge at an applied pressure of 0.479 kPa. Reprinted from Ballard et al. (2015), permission request pending.

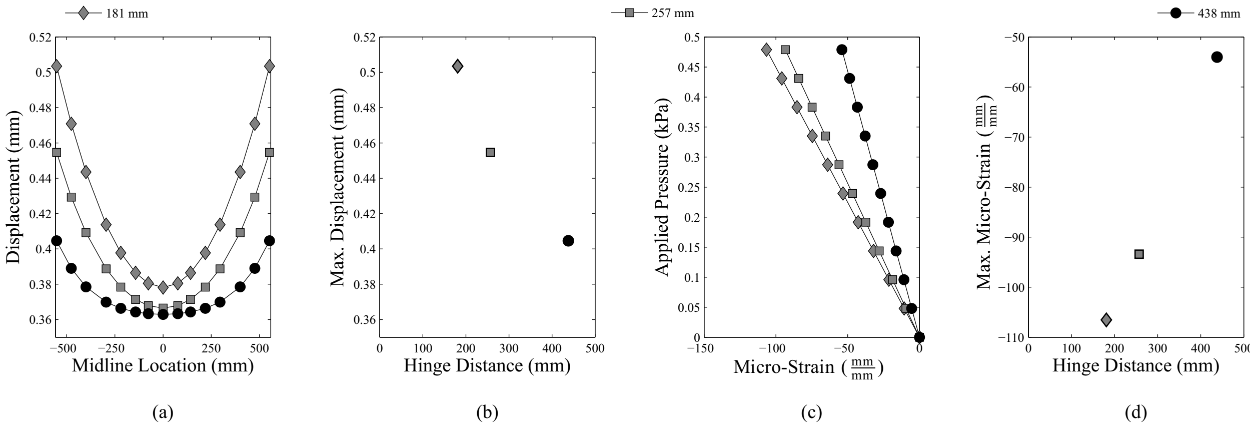

FIG. 7: Numerical behavior of panel (tension face) with varying hinge placement: (a) global displacements along panel midline at an applied pressure of 0.479 kPa, (b) maximum displacement at an applied pressure of 0.479 kPa, (c) longitudinal strain near hinge, and (d) maximum longitudinal strain near hinge at an applied pressure of 0.479 kPa. Reprinted from Ballard et al. (2015), permission request pending.